

Supporting Information

Spatially Selective Assembly of Quantum Dot Light Emitters in an LED *via* Decorating with Engineered Peptides

*Hilmi Volkan Demir¹, Urartu Ozgur Safak Seker^{1,4}, Gulis Zengin¹, Evren Mutlugun¹, Emre Sari¹,
Candan Tamerler^{2,3}, and Mehmet Sarikaya³*

¹Department of Electrical and Electronics Engineering, Department of Physics and UNAM - Institute of Material Science and Nanotechnology, Bilkent University, 06800 Ankara (Turkey)

²Molecular Biology and Genetics, MOBGAM, Istanbul Technical University, Maslak 34469, Istanbul, (Turkey)

³Genetically Engineered Materials Science and Engineering Center, Department of Materials Science and Engineering, University of Washington, Seattle, Washington 98105, USA

⁴*Luminous!* Center of Excellence for Semiconductor Lighting and Displays, School of Electrical and Electronic Engineering, Microelectronics Division; School of Physical and Mathematical Sciences, Physics and Applied Physics Division, Nanyang Technological University, 639798 (Singapore)

1. Preperation of Substrates and Specificty Experiments

We prepared Au/Silica and GaN/Silica samples for cross-specificity experiments. For the Au/Silica experiments, we prepared two different samples, one with silica patterns on the gold layer and the other with the gold patterns on silica layer. For Au/silica samples, we coated silicon substrate with 50 nm Ti, 500 nm Au and 50 nm Ti with a thermal evaporator (LH Leybold AG, Hanau, Germany and Inficon IC/4 Deposition Controller, East Syracuse, NY). Then, we deposited 300 nm thick silica using plasma enhanced chemical vapor deposition (PECVD) (Plasma Technology Plasmalab MicroP, Everet, WA) and then patterned different size squares (max. 300 nm along one side) using a mask aligner (Karl Suss MJB 3, Garching, Germany). Finally, we etched the silica with hydrofluoric acid (HF). Besides, the same samples were prepared by depositing 300 nm silica on silicon substrate and then 500 nm thick Au for subsequent lift-off to pattern the top gold film. For the GaN/silica sample, we deposited 300 nm

thick silica on GaN surface and then patterned it using mask aligner and etching. For the final step, we again etched silica with HF (hydrofluoric acid).

2. Fabrication of the LEDs

We used LED for the last part of the experiments. The LED epitaxial layers were grown by using a GaN dedicated metal–organic chemical vapor deposition (MOCVD) system (Aixtron RF200/4 RF-S, Aachen, Germany) at Bilkent University Nanotechnology Research Center. After deposition of a 14 nm thick GaN nucleation layer and a 200 nm thick GaN buffer layer, we grew a 690 nm thick, Si doped n-type contact layer and InGaN wells and GaN barriers as the active layers for 450 nm EL peak. As the final step, we grew p-type layers and GaN layers as the contact cap. During LED fabrication, standard semiconductor processes such as photolithography (Karl Suss MJB-3, Garching, Germany), thermal evaporator (LH Leybold AG, Hanau, Germany and IC/4 Plus Inficon Deposition Controller, East Syracuse, NY), and reactive ion etch (RIE) (LH Leybold AG, LE301, Hanau, Germany) and rapid thermal annealing (AG Associate Mini-Pulse, San Jose, CA) were used. The composition of n-contacts was 100 nm Ti and 2500 nm Al and then they were annealed at 600 °C for 1 min under N₂ purge. The p-contacts were composed of 15 nm Ni and 100 nm Au and were annealed at 700 °C for 30 s under N₂ purge. Next, 200 nm thick silicon oxide was deposited on the LEDs by using PECVD and then was etched by using RIE after a photolithograph process. Finally, QBP1-bio hybridized SA-QDots were incubated on the LEDs and washed with 500 μL buffer solution. Confocal microscopy (Carl Zeiss, LSM510 DuoScan, Thornwood, NY) was used to take images of SA-QDots on LED.

3. Assembly of quantum dots on color-conversion light emitting diodes

The streptavidin coated Evifluors Quantum Dot Conjugates were acquired from Evident Technologies (Troy, NY). A maple red-orange Quantum dot, with an emission peak at 620 nm was used. These QDots are first conjugated to PEG (polyethylene glycol) lipid Vitas, which have approximately 25 nm

hydrodynamic radius and have the characteristics of both multi-modal nanoparticles and fluorescent dye molecules. Then the QDots are activated with streptavidin molecules to couple with biotin. Approximately, one QDot contains 5 to 10 streptavidin molecules on its surface and its hydrodynamic radius increases up to 40 nm.

After combining QBP1-bio and SA-QDot solutions, the final solution was mixed in vortex mixer and then dropped to each quartz surface by using pipettes. After samples were incubated overnight in the incubation chamber, each quartz sample was washed with 500 μ L special buffer solution using pipettes. Next, the samples were dried by using nitrogen gun. The control samples were prepared similarly except that the nanocrystal solution was blended with the same volume of deionized water instead of blending peptide solution with the nanocrystal solution. Similarly, we washed the control samples with 500 μ L deionized water instead of buffer solution. The other preparation steps of control samples were identical to procedure described for the hybrid approach.

For the assembly experiments, equal volumes (15-30 μ L) of 100 μ g/mL peptide solutions and 2.5 μ M SA-QDots were used for each quartz chip with a size of 0.5 x 0.5 cm, similarly in the case of LED samples, the size of each LED devices was 300x300 μ m. The streptavidin coated nanocrystals were coated with biotinylated QBP1; this was achieved by optimizing the concentration and volume ratio of QBP1-bio and SA-QDots. Decorating the outer surface of SA-QDots with QBP1-bio makes SA-QDots easily bind to quartz surface.

The surface coverage of SA-QDots is different in sequential assembly and nano-hybrid assembly. Surface heterogeneity can possibly be effective during the sequential assembly of these SA-QDots on silica binding peptide decorated surface. This surface heterogeneity may be caused due to variations in the distribution of available biotins on the silica surface. The distribution of biotins on the silica surface may change locally from region to region on the substrate as a result of the surface diffusion of the peptides, which has been reported previously for solid binding peptides.¹ Another possibility is that, although the silica binding peptides are homogeneously adsorbed on the silica surface, the biotins may

not be exposed freely depending on the mode of conformation of the QBP1-bio in the adsorbed state. Thus, while some of these biotins might be exposed, some might not be. This can cause a decrease in the number of available biotin sites, which -including surface heterogeneity- has also been reported earlier as a possible reason for mass transport limitation.^{2, 3} Additionally, in previous studies, possible steric hindrances between biotinylated molecules and streptavidin were discussed in detail and taken under consideration as possible reasons for mass transfer limitation, although it was also reported that steric hindrances may not be significant according to one study.⁴ One may argue the possibility of quenching of quantum dots on a gold film due to possible plasmonic coupling. If a plasmonic structure couples with a luminescence structure, it may lead to quenching or enhancement of emission. This depends on the spectral and spatial conditions. In case of a metal nanoparticle, if the plasmonic resonance of the nanoparticle overlaps with the emission wavelength of the QDot, then one can facilitate plasmon coupling. In our case we have a flat gold film with a thickness of 500 nm. For this film thickness, the flat gold film does not have a plasmon resonance at the emission wavelength of QDots. Thus it cannot plasmon couple with QDots. However a metal film can help with reflection of the emitted light from QDots. It may sure as a good reflector. Another possibility for quenching may be the charge transfer in general. However in the case of these QDots we have three monolayers of ZnS barrier which enables electrostatically full isolation. This means all the electron and hole wave functions are fully confined within the CdSe, and there cannot be a charge transfer. Neither Au substrate nor GaN substrate quench QDots. With a control experiment we tested the above argued fact about the possibility of quenching of QDot on metallic surfaces due to the plasmonic coupling. In Figure S1, the intensity of QDots on GaN, silica and gold were recorded. As explained above QDots does not quench neither on gold nor on GaN.

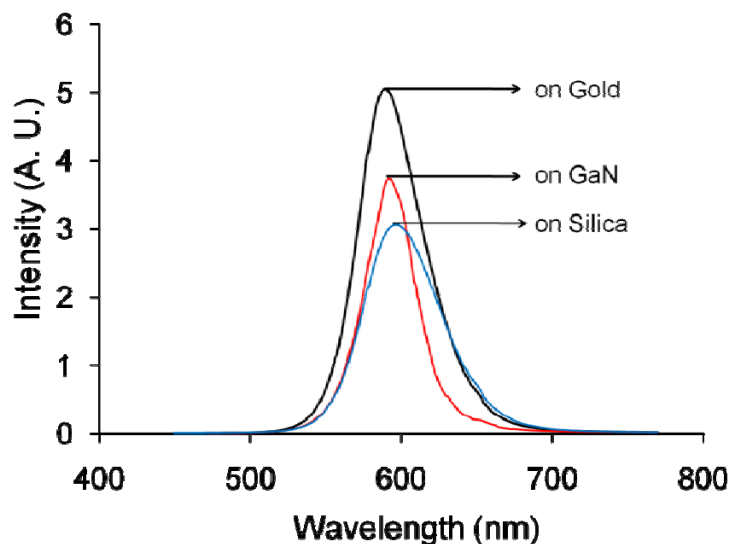


Figure S1. Comparison of photoluminescence of QDot on gold, GaN and silica surfaces

4. Electroluminescence of SA-QDOT+QBP1-bio hybridized LED Device:

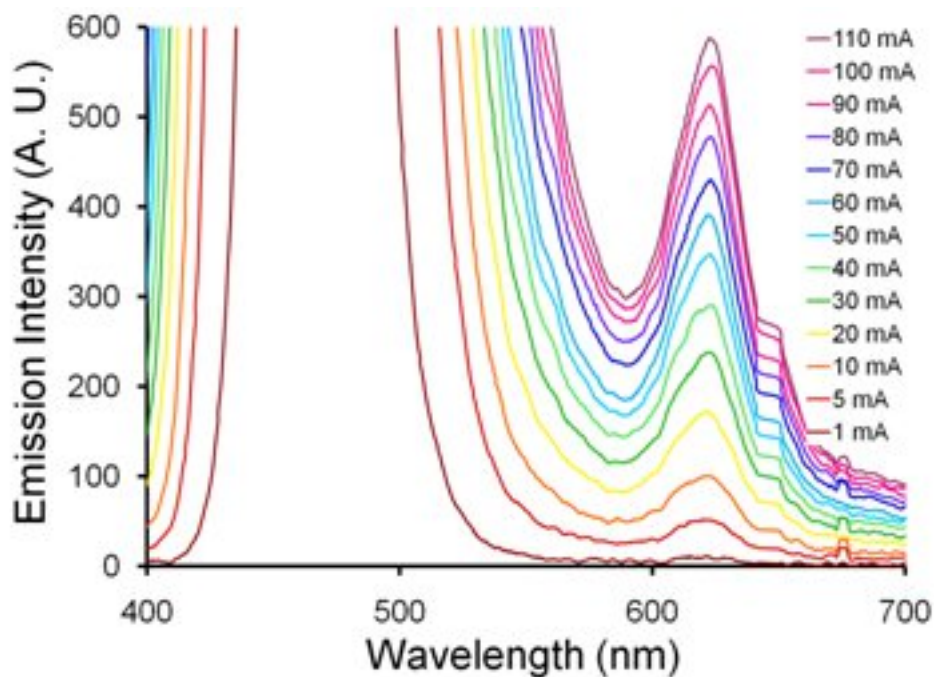


Figure S2. Full Wavelength data of Photoluminescence of the hybrid construct targeted-assembled on the silica that is optically pumped by the electrically driven LED at room temperature

5. Surface plasmon resonance (SPR) spectroscopy experiments

Adsorption of small molecules on solid substrates (e.g., Au) can be monitored using surface plasmon

resonance spectroscopy.⁵ The measurements yield both the adsorption and desorption constants and binding energy. The SPR experiments were carried out using a configuration and experimental method discussed in our previous work.^{6, 7} The SPR measurements were recorded at 27 ± 0.1 °C using a temperature controller system and the solutions used in these experiments were flowed through the apparatus using a peristaltic pump (80 μ L/min), and switching between different solutions was achieved via the use of a 6-port valve (Upchurch Scientific). To establish a baseline for experimental measurements, solutions containing buffer alone were first flowed through the apparatus and coated slide. Next, buffer solutions containing each peptide (0.7, 1.7, 5.1 μ M final peptide concentrations) were introduced. After a specified interval to allow peptide adsorption onto the silica thin films, a solution consisting of buffer minus peptide was flowed through the system to monitor peptide desorption from the target thin film. The SPR data were collected using WinSpectral 1.03 software, which measures the normalized dip spectrum at periodic intervals (Figure S1). The dip is fitted to a 4th degree polynomial function for generating the time-dependent metric sensogram. The conventional gold SPR substrate was coated with 10 nm of silica layer on top of the gold; each of the experiments were carried out using a slide for one time. The calculation of the adsorption of QBP1-bio on silica surface was made using a modified Langmuir adsorption model.^{6, 7} We discussed the details of the calculation that adsorption isotherms from the experimental data were fitted using the single Langmuir⁵ or modified (*i.e.*, bi-exponential) Langmuir adsorption models. The single isotherm is described by Equation (1).

$$\frac{d\theta}{dt} = k_a(1-\theta)C - k_d\theta \quad (1)$$

Here, θ is the fraction of the available sites that are covered; k_a , and k_d are the association and dissociation rate constants, respectively; and C is the peptide concentration (molar units). The integration of Equation (1) then yields the description of the change in time-dependent monolayer coverage given in Equation (2).

$$\theta(t) = \frac{C}{C + (k_d / k_a)} [1 - \exp(-(k_a C + k_d)t)] \quad (2)$$

For a given time period and temperature, monolayer formation can be described as a function of time by a single rate constant, called k_{obs} , where $k_{obs} = k_a C + k_d$. The rate constant k_{obs} represents both the adsorption and desorption coefficients as a function of peptide concentration. Substituting this expression in Equation (2) along with the expression for surface coverage $\theta(\infty) = C / [C + (k_d / k_a)]$ leads to Equation (3).

$$\theta(t - t_0) = \theta(\infty) [1 - \exp(-k_{obs}(t - t_0))] \quad (3)$$

Equation (3) describes the single Langmuir isotherm model. However, we realize that not all protein adsorption processes can be described by this model as many biomolecular reactions at interfaces are more complex. For example, in the bi-exponential process, protein adsorption onto a surface involves two events, or stages, often simultaneously, that are governed by different rate constants. We modified Equation (4) to reflect the overall observed adsorption process with two different rates; here, the total fractional surface coverage can be represented in Equation (4):

$$\theta_{obs}(t) = x_1 \theta_1(t) + x_2 \theta_2(t) = x_1 \theta_1(\infty) (1 - \exp(-k_{obs}^1 t)) + x_2 \theta_2(\infty) (1 - \exp(-k_{obs}^2 t)) \quad (4)$$

where, $k_{obs}^1 = k_a^1 C + k_d^1$ and $k_{obs}^2 = k_a^2 C + k_d^2$ represent the two different stages of the adsorption process at the surface.^{6, 7} As a consequence of Equation (4), we observe two different rate constants and two different association and dissociation constants. The adsorption process happens at faster and slower rates. These two different (fast and slow) adsorption behaviors can be triggered by the heterogeneity of the surface structure of the inorganic surface, the conformational change of the peptide during adsorption. Another possible explanation of two different adsorption rates is attributed to the mass transfer limitation.^{8, 9} In Figure S1 the fitted lines for the calculation of the K_{eq} of QBPI is given

as inset, also the calculated surface coverage of QBP1 as a function of concentration is given.

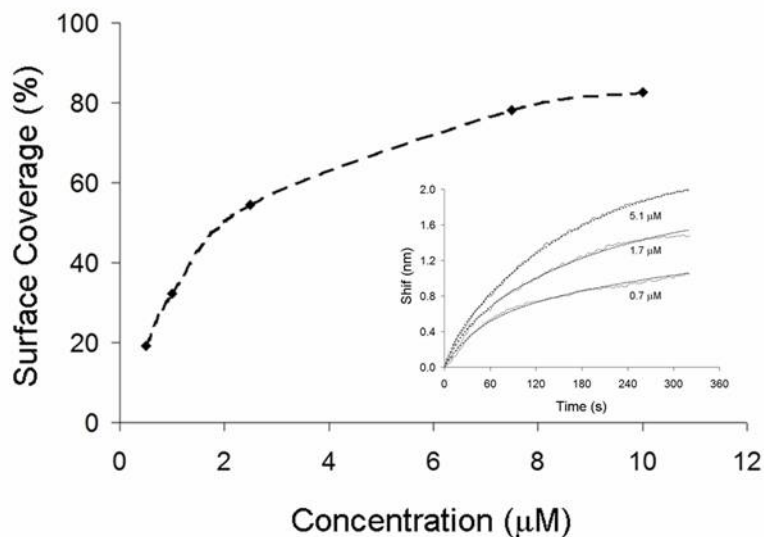


Figure S2. Langmuir calculations using modified Langmuir isotherms, with the inset graph showing the adsorption isotherms for the binding of QBP1-bio on a silica surface.

References:

- (1) So, C. R., Tamerler, C., Sarikaya, M. Molecular Recognition and Supramolecular Self-Assembly of a Genetically Engineered Gold Binding Peptide on Au{111}. *Angew. Chem. Int. Ed.*, **2009**, 28, 5174-5177.
- (2) Jung, L. S., Nelson, K. E., Stayton, P. S., Campbell, C. T. Binding and Dissociation Kinetics of Wild-Type and Mutant Streptavidins on Mixed Biotin-Containing Alkylthiolate Monolayers *Langmuir*, **2000**, 24, 9421-9432.
- (3) Jung, L. S., Nelson K. E., Campbell C. T., Stayton P. S., Yee S. S., Pe´rez-Luna V., Lo´pez G. P., Surface Plasmon Resonance Measurement of Binding and Dissociation of Wild-Type and Mutant Streptavidin on Mixed Biotin-Containing Alkylthiolate Monolayers. *Sens. Actuators*, **1999**, 137–144.

- (4) Wenmiao Shua, Ernest D. Laue, Ashwin A. Seshia, Investigation of Biotin–Streptavidin Binding Interactions Using Microcantilever Sensors. *Biosens. Bioelect.*, **2007**, 2003–2009
- (5) Karpovich, D.S.; Blanchard, G.J. Direct Measurement of the Adsorption Kinetics of Alkanethiolate Self-Assembled Monolayers on a Microcrystalline Gold Surface. *Langmuir* **1994**, *10*, 3315-3322
- (6) Tamerler, C.; Oren, E. E.; Duman, M.; Venkatasubramanian E.; Sarikaya, M. Adsorption Kinetics of an Engineered Gold Binding Peptide by Surface Plasmon Resonance Spectroscopy and a Quartz Crystal Microbalance. *Langmuir* **2006**, *22*, 7712-7718
- (7) Seker, U. O. S.; Wilson, B., Dincer, S.; Evans, J. S.; Oren, E. E.; Tamerler, C.; Sarikaya, M. Adsorption Behavior of Genetically Engineered Linear and Cyclic Pt-Binding Peptides. *Langmuir* **2007**, *23*, 7895-7900.
- (8) Glaser, R. W. Antigen-Antibody Binding and Mass Transport by Convection and Diffusion to a Surface: A Two-Dimensional Computer Model of Binding and Dissociation Kinetics *Anal. Biochem.* **1993**, *213*, 152–161.
- (9) Schuck, P. Kinetics Of Ligand Binding To Receptor Immobilized in A Polymer Matrix, as Detected with an Evanescent Wave Biosensor. I. A Computer Simulation of the Influence of Mass Transport *Biophys. J.* **1996**, *70*, 1230–1249.